

Relationships between Climate Variability and Winter Temperature Extremes in the United States

R. W. HIGGINS, A. LEETMAA, AND V. E. KOUSKY

Climate Prediction Center, NOAA/NWS/NCEP, Washington, D.C.

(Manuscript received 10 January 2001, in final form 28 October 2001)

ABSTRACT

Time series representing two of the climate systems leading patterns of variability, namely El Niño–Southern Oscillation (ENSO) and the Arctic Oscillation (AO), are used together with 50 yr of daily mean surface air temperature data over the conterminous United States to diagnose relationships between winter temperature extremes and interannual climate variability. The aim is to focus attention on some of the physical phenomena that climate models must be able to simulate in order to be deemed credible for use in weather and climate forecasts and assessments.

Since the 1950s there has been considerable decadal variability in winter surface air temperature extremes. At most locations in the United States the number of daily extremes is reduced during El Niño, and increased during La Niña and ENSO-neutral years. These changes are qualitatively consistent with a decrease in the daily mean surface air temperature variance during El Niño relative to La Niña and ENSO neutral.

Changes in the number of warm extremes during a particular AO phase are largely compensated for by changes in the number of cold extremes, so that the net change in the numbers of surface air temperature extremes is close to zero. However, the AO is associated with larger changes in mean temperature than ENSO.

1. Introduction

It is increasingly clear that a better understanding of the linkages between weather and climate is needed since many decision-making processes are directly tied to weather “events.” It is the yet largely unexplained relationships between extreme weather events, climate variability, and long-term trends that are likely to have the most direct impacts on society (e.g., Pan et al. 1995; Brown et al. 1986). A better understanding of these relationships will only come from additional diagnostic studies and numerical experimentation.

Understanding relationships between climate variability and extreme weather events is made difficult by mutual interactions between these two characteristics of climate. For example, climate variations are manifested as changes in the large-scale atmospheric and/or oceanic circulation patterns. These cause shifts in the temperature and precipitation probability distribution functions (PDFs); that is, shifts toward wetter/drier/warmer/cooler conditions, by either causing a shift in the mean of the PDF and/or by changing its shape (i.e., variance). Both effects magnify the changes in the probability of extreme events on the tails of the distribution.

Several previous studies have described the effect of ENSO on the U.S. *seasonal* and *monthly* average temperatures (e.g., Ropelewski and Halpert 1986, 1996; Redmond and Cayan 1994). The effect of ENSO on the probability distribution of *daily* surface air temperature over the Pacific–North American sector has been investigated using National Centers for Environmental Prediction–National Center for Atmospheric Research (NCEP–NCAR) reanalysis data (Smith and Sardeshmukh 1999); and in observations and general circulation model output (Gershunov and Barnett 1998). All of these studies point to the fact that large regions of the United States experience significant modulation of winter temperature by ENSO.

It is likely that from a priori principles it will be difficult to accurately assess the characteristics of extreme weather events under different climate regimes because the mean conditions and extreme events during a season are the result of contributions from a number of factors, which can act independently, and which may not be predictable (i.e., in an initial value problem). Possible contributors include the leading patterns of climate variability [e.g., ENSO, the Arctic Oscillation (AO), the Pacific Decadal Oscillation (PDO), etc.], and long-term trends possibly related to global climate change. One way to start to approach this problem is to isolate the contributions of the leading patterns of climate variability, which are linked to changes in the large-scale circulation of the atmosphere. This approach

Corresponding author address: Dr. R. W. Higgins, Analysis Branch, Climate Prediction Center, NOAA/NWS/NCEP, 5200 Auth Rd., Room 605A, Camp Springs, MD 20746.
E-mail: Wayne.Higgins@noaa.gov

TABLE 1. Datasets used in this study.

Field	Resolution	Period of record	Source
U.S. surface air temperature	0.5° × 0.5°	1948–99	Janowiak et al. (1999), NCDC “Coop Summary Of the Day”
Sea surface temperature	2.0 × 2.0	1950–99	Reynolds and Smith (1995) Smith et al. (1996)
Geopotential height, winds, sea level pressure	2.5° × 2.5°	1948–99	Kalnay et al. (1996) NCEP–NCAR reanalysis

has been used to examine the predictability of U.S. precipitation and surface air temperature (e.g., Higgins et al. 2000). The use of decadal trends in seasonal forecasting is also currently employed by the Climate Prediction Center. Using rotated canonical correlation analysis between U.S. surface temperature and global SST, Livezey and Smith (1999) identified two signals with considerable variance on interdecadal or longer time-scales. They showed that the associated upper-air circulation patterns have significant projections on the Pacific–North America (PNA) pattern and the North Atlantic Oscillation (NAO).

It is a specific goal of this study to diagnose how the leading patterns of interannual *climate variability* are related to daily *temperature extremes*. These relationships are diagnosed using daily mean surface air temperature data for the conterminous United States during the 50-yr winter period [January–February–March (JFM) 1950–99]. Because our daily time series is too short to disentangle decadal climate variability, we will not consider relationships between the leading patterns of decadal *climate variability* (e.g., PDO, Atlantic multidecadal variability, etc.) and daily *temperature extremes* in this study. Daily temperature extremes are defined as those in the upper and lower 10% of the daily mean surface air temperature distribution, in accordance with the Intergovernmental Panel on Climate Change (IPCC) Third Assessment Report (Houghton et al. 2001). The aim of this study is to focus attention on some of the physical phenomena that climate models must be able to simulate (in an initial value problem) in order to be deemed credible for use in weather and climate forecasts and assessments.

It is the National Oceanic and Atmospheric Administration’s (NOAA’s) responsibility to provide the United States with the best possible guidance regarding future climate variations and trends. Integrated modeling, that is, modeling that brings together the climate and weather communities, will serve as a primary tool with which to create the necessary products. Yet at the present time the weather and climate modeling communities are not sufficiently coordinated to ensure technology transfer between the efforts. It is our aim to demonstrate that linkages between interannual climate variability and weather extremes are pervasive in the observations, and hence that stronger collaboration between the modeling communities is needed.

This study emphasizes daily mean surface air tem-

perature extremes during Northern Hemisphere winter (January–March), since this is the time of year when climate variability is strongly related to weather extremes. The datasets and methodology are described in section 2. The leading patterns of climate variability (i.e., ENSO and the AO) are briefly reviewed in section 3. Surface air temperature patterns and numbers of temperature extremes are examined by decade in section 4. Standardized indices representing ENSO, and the AO are used together with composite analysis to relate interannual climate variability to temperature extremes in section 5. A discussion is presented in section 6.

2. Data analysis

The study examines 50 years (JFM 1950–99) of daily mean surface air temperature data (Janowiak et al. 1999) over the conterminous United States (see Table 1 for additional information on this dataset and other datasets used in this study). Here daily mean surface air temperature is obtained by averaging daily maximum and daily minimum temperature. Warm and cold extremes are defined as the upper and lower 10% of the days, respectively. Because we are working with winter temperature extremes, we refer to them as *warm* and *cold*. Unless otherwise noted the terms surface air temperature and temperature are used interchangeably in this study.

In order to ensure that all warm extremes are not in March and all cold extremes are not in January, the daily data have a smooth annual cycle (defined as mean daily values for each day of the year) removed from them. The time mean removed from the daily data is for the full 50-yr (1950–99) period. An examination of the local distributions of warm and cold extremes by date for the 1950–99 period (not shown) reveals that both warm and cold extremes are almost uniformly distributed (i.e., on the order of five warm and five cold extremes per date). Since the standard deviation and skewness vary with the seasonal cycle, the occurrence of extreme days is slightly non uniform.

A Student’s *t* test was used to evaluate the statistical significance of surface air temperature anomalies (Figs. 4 and 9) and skewness (Fig. 13). The test was also used to evaluate the statistical significance of departures from the average number of extremes per winter (as defined in section 4b in Figs. 5–7, 10 and 12, and in Table 2).

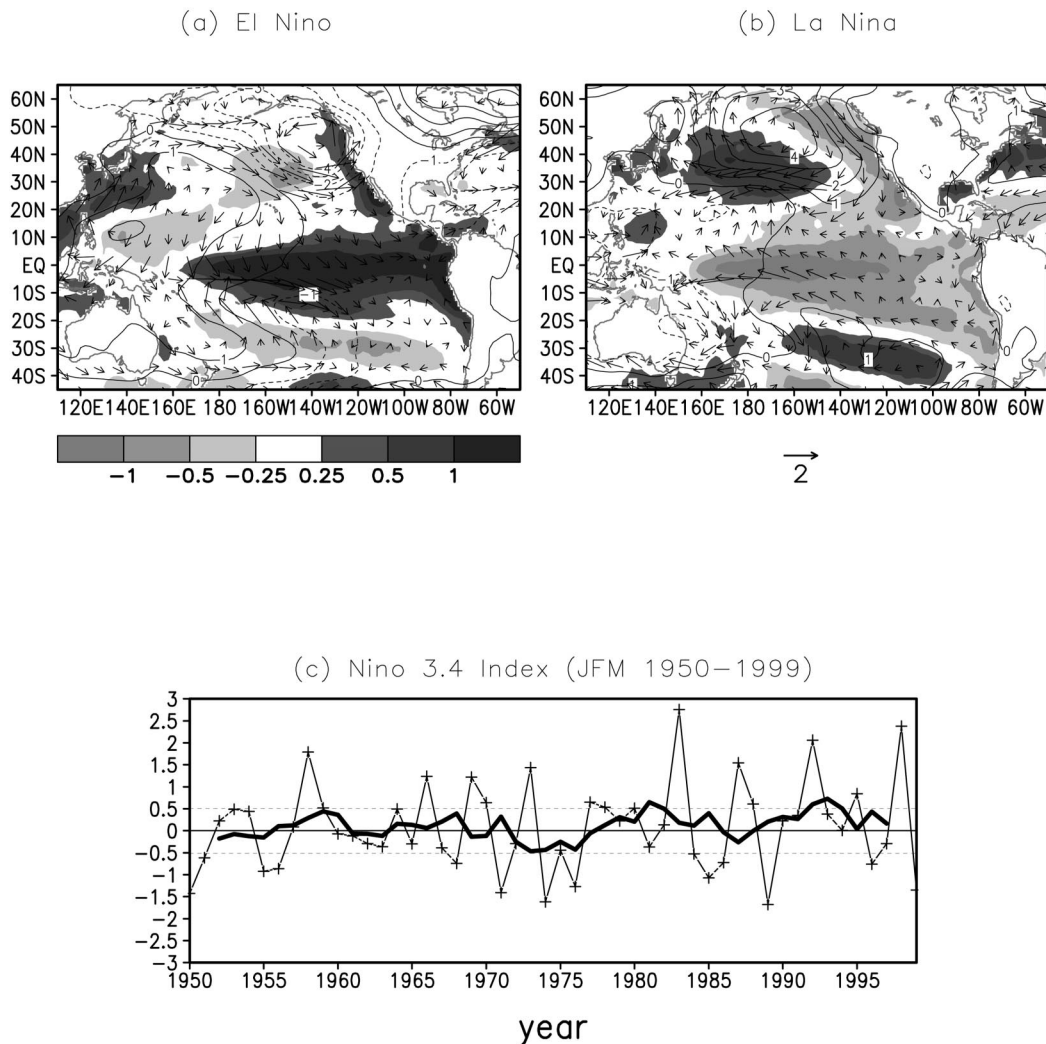


FIG. 1. Typical wintertime (JFM) sea surface temperature anomalies (shading; $^{\circ}\text{C}$), SLP anomalies (contours; hPa) and 10-m wind anomalies (m s^{-1}) during (a) El Niño and (b) La Niña. The standard vector length is 2 m s^{-1} . Anomalies are departures from 1950 to 1999 base period monthly means. SLP and wind data are from the NCEP–NCAR reanalysis and SST data are from the analysis of Reynolds and Smith (1995). (c) Standardized (unit std dev) Niño-3.4 SST index for JFM 1950–99.

In each case statistical significance was assessed relative to the 95% confidence level.

In this study we examine extremes for January–March together, but acknowledge that it would also be interesting to examine January–February–March separately. In section 5b, the intraseasonal (i.e., timescales less than 90 days) component of the total variance is computed by first removing the seasonal mean for each year from the daily data. In section 4 the 50-yr (1950–99) linear trends are estimated by least squares fits using seasonal mean data.

3. The leading patterns of climate variability and their impacts

The leading patterns of climate variability can be viewed as building blocks to progress in climate fore-

casting, at least for relatively short (i.e., intraseasonal-to-interannual) timescales. The El Niño–Southern Oscillation (ENSO) phenomenon is the major source and best understood pattern of interannual climate variability (Fig. 1). El Niño episodes (also called Pacific warm episodes or ENSO) and La Niña episodes (also called Pacific cold episodes) represent opposite extremes of the ENSO cycle. El Niño features two prominent changes in the atmospheric flow across the eastern North Pacific and North America (Fig. 2b). The first is a flattening of the climatological mean wave pattern and much more zonally uniform flow than normal across the entire eastern North Pacific and North America. The second is a pronounced eastward extension and equatorward shift of the Pacific jet stream (Bell and Kousky 1995) to the southwestern United States. Accompanying

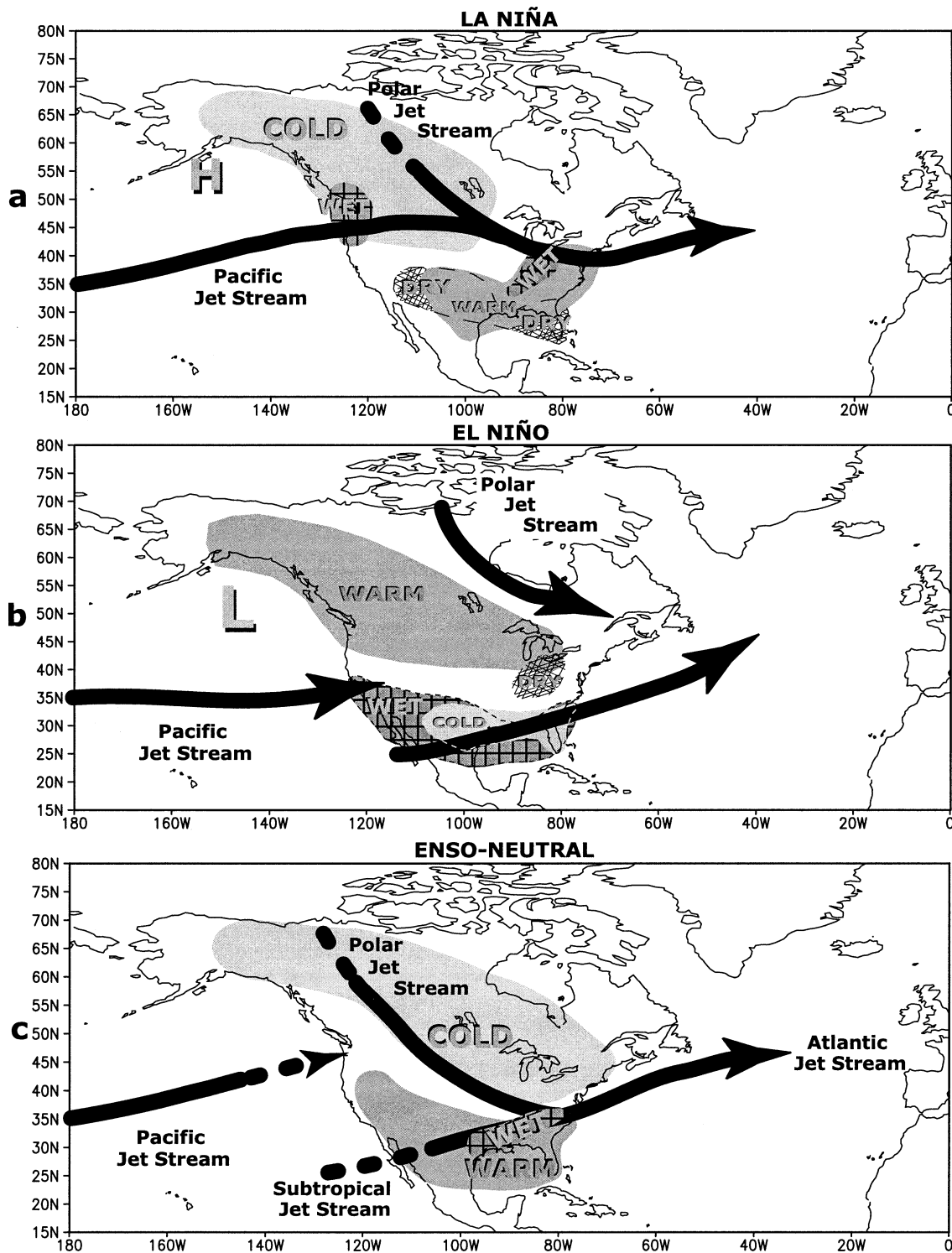


FIG. 2. Typical winter patterns associated with (a) La Niña, (b) El Niño, and (c) ENSO-neutral conditions. The composite anomalies shown are based on 14 La Niña, 18 El Niño, and 18 ENSO-neutral winters during the JFM 1950–99 period.

this flow pattern, midlatitude low pressure systems tend to be more vigorous than normal over the eastern North Pacific and the southern tier of the United States. Also, there is an enhanced flow of Pacific maritime air into most of North America, and a reduced northerly flow of cold air from Canada to the United States, resulting in a milder than normal winter across the northern tier of the United States and western Canada (Fig. 2b).

La Niña episodes feature three prominent changes in the atmospheric flow across the eastern North Pacific and North America (Fig. 2a). The first is an amplification of the climatological mean wave pattern and increased meridional flow across the continent and the eastern North Pacific. The second is increased blocking activity across the eastern North Pacific. The third is increased variability in the strength of the Pacific jet stream over the eastern North Pacific, with the mean jet position entering North America in the northwestern United States/southwestern Canada. Accompanying these conditions, large portions of central North America experience increased storminess, increased precipitation, and cooler than normal conditions (Fig. 2a). In contrast, the southern tier of the United States experiences less precipitation, and is warmer than normal. Also, there tends to be considerable month-to-month variation in temperature, and precipitation across central North America during the winter in response to the more variable atmospheric circulation.

ENSO-neutral winters feature a weakening of the Pacific jet stream as it approaches the west coast of North America (Fig. 2c). These winters are also characterized by active polar and subtropical jet streams extending over the North American continent, consistent with an increase in day-to-day (temperature and precipitation) variability (see section 5). In the confluence between these two streams there is enhanced storminess resulting in above-normal precipitation (Fig. 2c). ENSO-neutral winters also feature cooler than normal conditions on the poleward side of the polar jet stream and warmer than normal conditions along the southern tier of the United States.

The dominant mode of variability in the Northern Hemisphere (NH) extratropics is the AO, which Thompson and Wallace (1998, 2000) have shown to be the primary mode of wintertime variability on timescales ranging from intraseasonal to interdecadal. The AO incorporates many of the features of the associated, more localized NAO (e.g., Walker and Bliss 1932; van Loon and Rogers 1978; Hurrell 1995) but its larger horizontal scale and higher degree of zonal symmetry render it more like a surface signature of the polar vortex aloft. The NAO may be viewed as the regional expression of the AO in the Atlantic sector (Wallace 2000). Thompson and Wallace (1998) showed that the AO accounts for a substantially larger fraction of the variance of NH surface air temperature than the NAO.

The AO is marked by opposing fluctuations in barometric pressure over the polar cap region and the mid-

latitudes (Fig. 3), together with opposing fluctuations in the strength of the westerlies at subpolar and subtropical latitudes (Thompson and Wallace 1998, 2000). It has far reaching effects on winter weather over the United States, Europe, and Asia, and it appears to amplify with height from the troposphere into the lower stratosphere (Thompson and Wallace 2000). Over the past 30 years it has exhibited a pronounced trend (Thompson and Wallace 1998) that has favored milder winters over Europe, Siberia, eastern Asia, and the contiguous United States. At present there is not a consensus in the climate community on whether this trend is a forced response (e.g., to changes in the radiative forcing) and/or natural variability.

In this study standardized (unit standard deviation) seasonal values of the ENSO, and AO indices are used for the period JFM 1950–99 (see Figs. 1c and 3c, respectively). The ENSO, and AO indices were used to construct the composites shown in Figs. 1a,b and 3a,b, respectively. High (low) index phases of each mode are deemed to occur when the appropriate index exceeds +0.5 (–0.5) standard deviations. The Niño-3.4 index used in many studies for ENSO yields a classification of El Niño and La Niña events during boreal winter (defined here as JFM) that is identical to that used by the Climate Prediction Center (CPC) and found on their Web site (http://www.cpc.ncep.noaa.gov/research_papers/ncep_cpc_atlas/8/ensoyrs.txt); we note that the Niño-3.4 and CPC classifications are not identical in other seasons, notably boreal summer. The sea surface temperature data used to generate the ENSO index is from Reynolds and Smith (1995) and Smith et al. (1996). The AO index was kindly provided by D. Thompson (Thompson and Wallace 1998). It was defined on the basis of the standardized leading principal component time series of monthly mean NH sea level pressure (SLP) for all months of the year. Previous studies have shown that the AO exhibits considerable variability on timescales less than a season. Finally, we note that the ENSO and AO indices are not significantly correlated ($r = -0.10$) during the 50-yr period under investigation in this study.

4. Characteristics of U.S. surface air temperature

At many locations in the United States (especially near the midlatitude jet stream) the daily mean surface air temperature distribution resembles a normal distribution, where nonstationarity of the distribution implies changes in the mean or variance. In such a distribution an increase in the mean leads to new record high temperatures, but a change in the mean does not imply any change in variability. On the other hand, an increase in the variability without a change in the mean implies an increase in the probability of temperatures on both tails of the distribution as well as the absolute value of the extremes. For instance, when variability increases and the mean changes (i.e., increases or decreases), the fre-

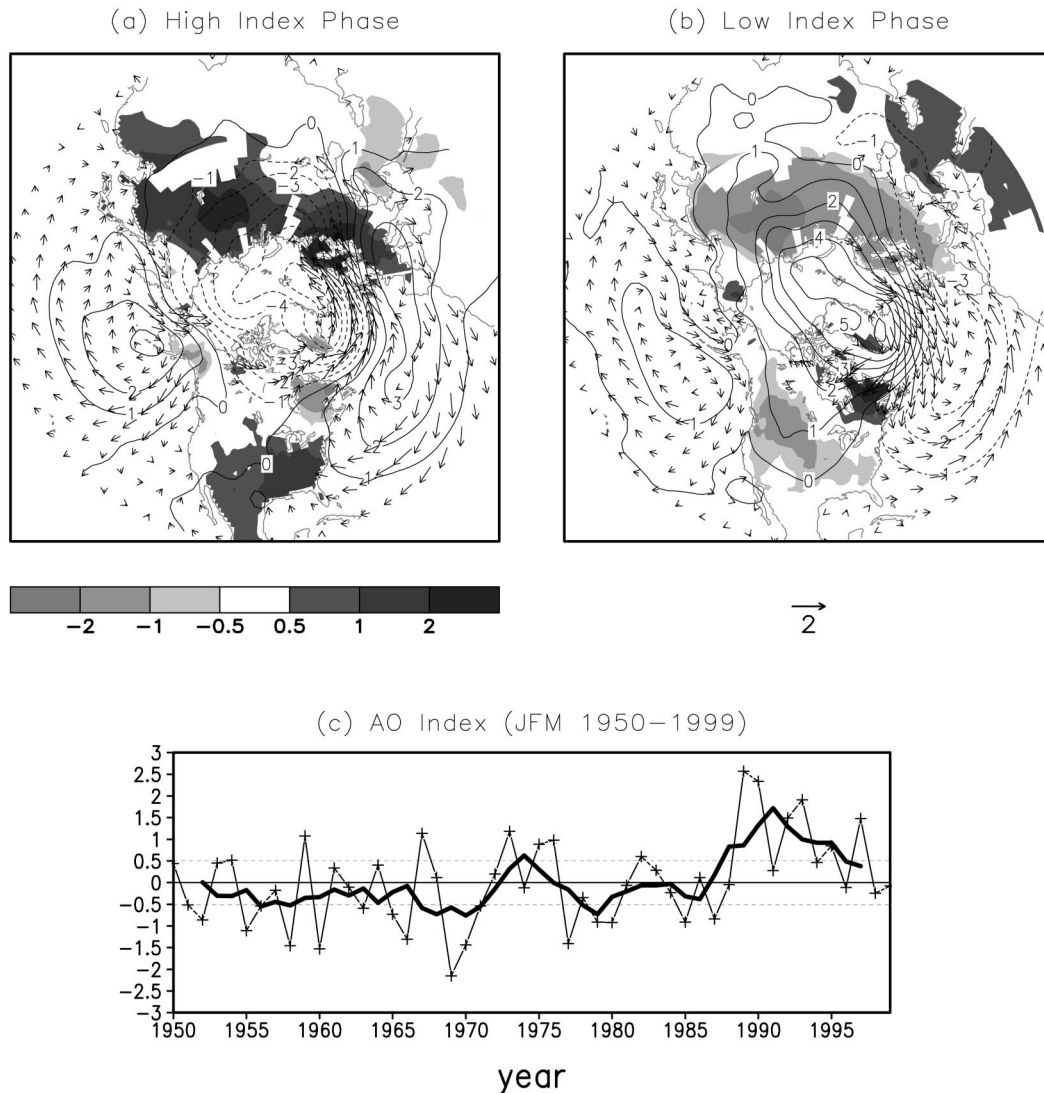


FIG. 3. Typical wintertime (JFM) surface air temperature anomalies (shading: °C), SLP anomalies (contours; hPa) and 10-m wind anomalies (m s^{-1}) during the (a) high-index phase and (b) the low-index phase of the AO. The standard vector length is 2 m s^{-1} . Anomalies are departures from 1950 to 1999 base period monthly means. SLP and wind data are from the NCEP–NCAR reanalysis and surface air temperature anomalies are from Jones (1994). (c) Standardized (unit std dev) AO index (Thompson and Wallace 1998) for JFM 1950–99. The high- (low-) index phase of the AO occurs when the AO index exceeds $+0.5$ (-0.5) std dev.

quency of occurrence of temperature extremes in one or both tails of the distribution is affected.

a. Decadal changes in temperature

Since 1950 there has been considerable decadal variability in U.S. winter surface air temperature with marked regional variability (Fig. 4). During the 1950s, temperatures were cooler than normal in the northwest and warmer than normal in the southeast. This pattern was dominated by the strong La Niña episode during the mid-1950s. From the 1950s to the 1960s, temperatures decreased over much of the United States, except

in the West. During the 1970s, winter temperatures remained cooler than normal over much of the United States, but temperatures warmed slightly across the southern tier of states relative to the 1960s. Further inspection of the temperature distribution for individual years during the 1970s (not shown) indicated that very cold weather during the *late* 1970s, especially over the northern United States, dominated relatively warm weather that occurred during the *early* 1970s (in association with the 1972/73 El Niño). Since the 1970s, there have been substantial increases in winter temperatures. The 1980s featured warmer than normal temperatures in the northern Great Plains and cooler than normal

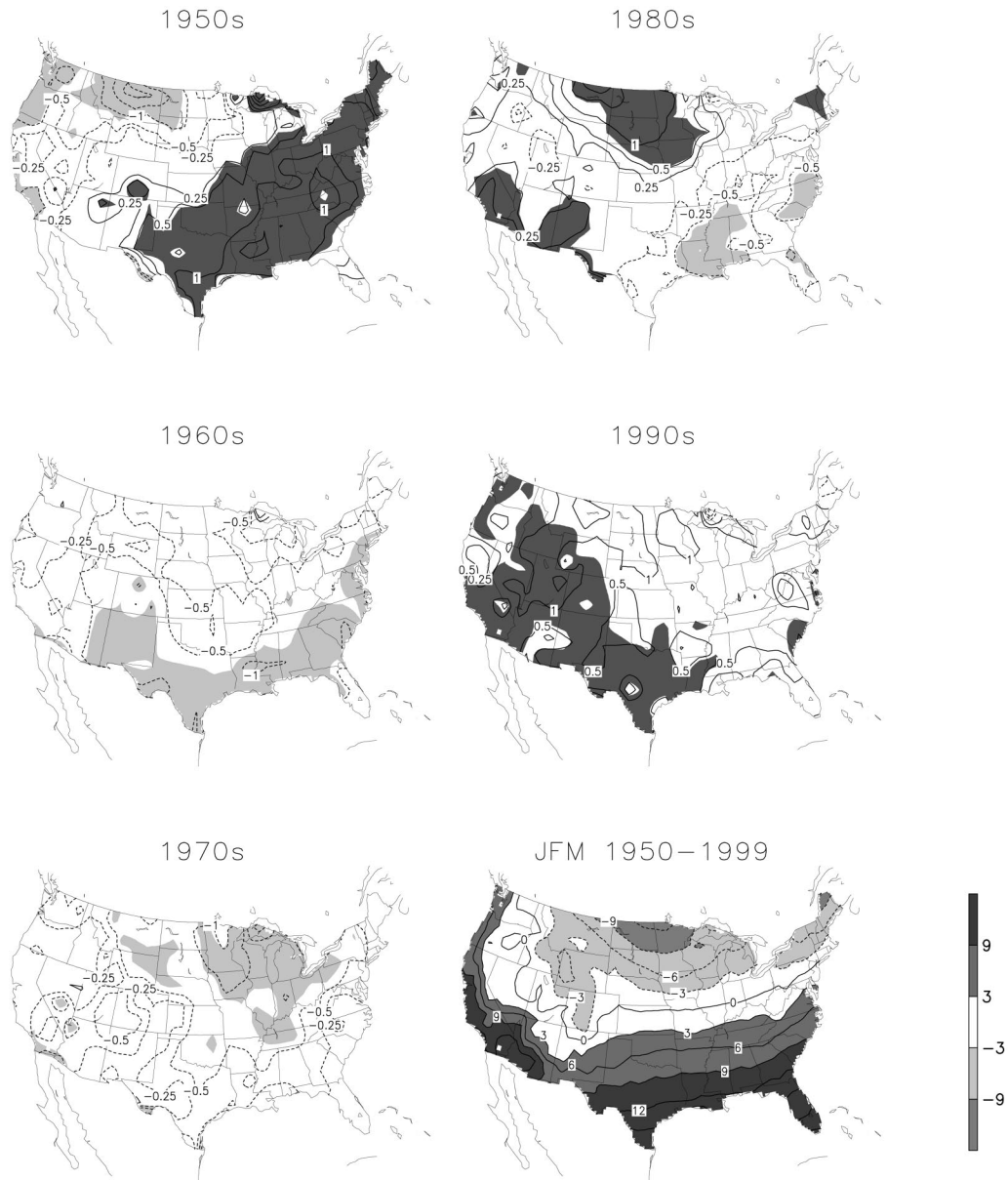


FIG. 4. Surface air temperature anomalies ($^{\circ}\text{C}$) during NH winter (JFM) in the 1950s, 1960s, 1970s, 1980s, and 1990s. Temperature anomalies are referenced to a JFM 1950–99 base period. Dark (light) shading indicates positive (negative) anomalies significant at the 95% confidence level. Climatological mean winter temperatures ($^{\circ}\text{C}$) for JFM 1950–99 are shown in the lower-right panel.

conditions in the Southeast, while the 1990s featured warmer than normal conditions over much of the conterminous United States, especially in the Southwest. For the conterminous United States, mean temperatures were warmest during the 1990s and coolest during the 1960s.

b. Numbers of extreme events

Daily-mean surface air temperature data were ranked (locally) at each grid point on a $0.5^{\circ} \times 0.5^{\circ}$ lat–lon grid

from the warmest day to the coldest day for the period JFM 1950–99. Warm (cold) days were defined as those in the upper (lower) 10% of the distribution. Thus, if warm and cold days were randomly distributed, then this implies that 9 warm (cold) days would occur, on average, at a particular location during a 90-day winter. Warm (cold) extremes were then stratified by decade to determine the number of extremes in each decade. Spatial patterns of the number of warm, cold, and warm plus cold days per decade are shown in Figs. 5–7. Dark (light) shaded areas indicate where the number of ex-

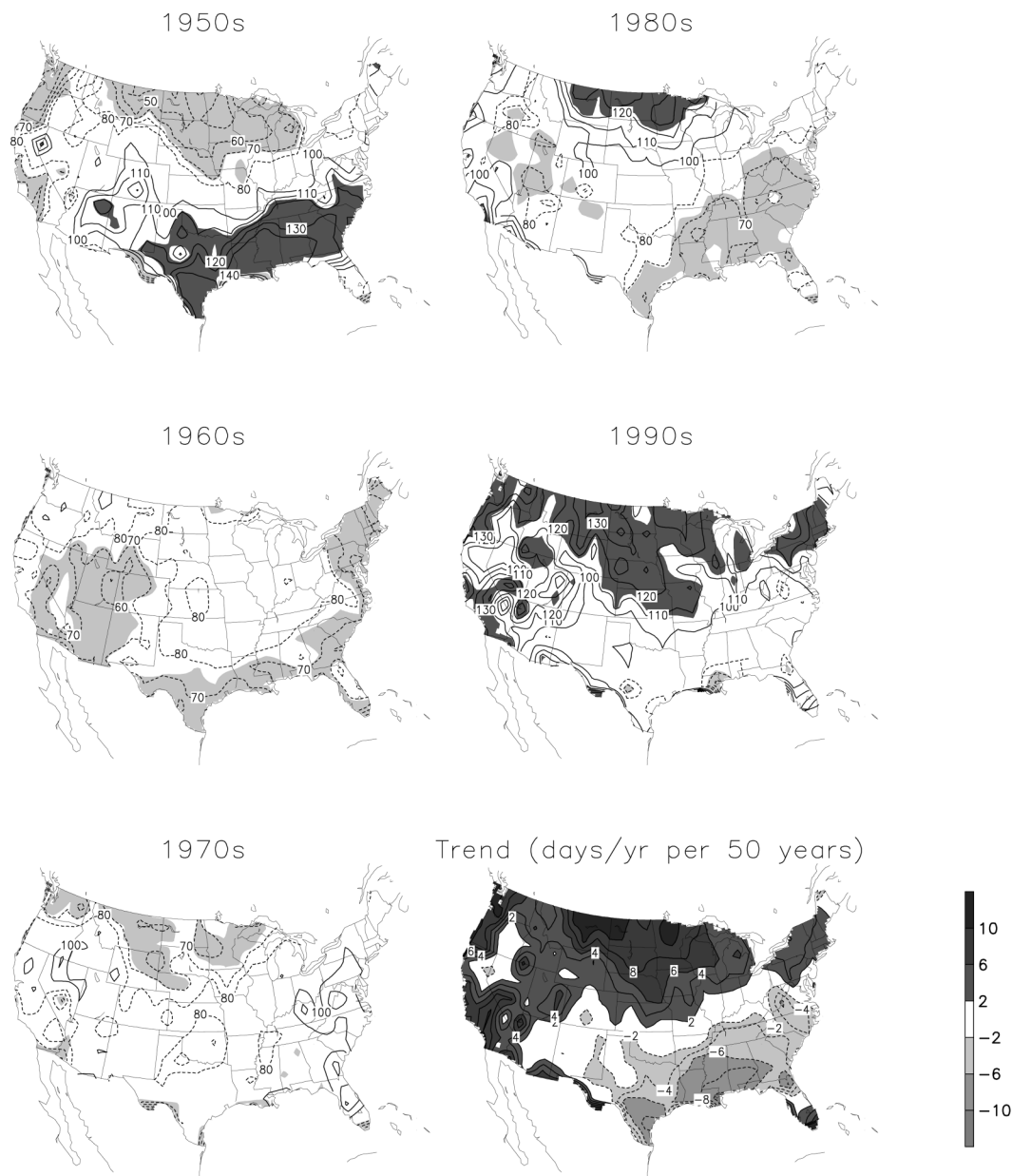


FIG. 5. Number of warm days that occurred during the 1950s, 1960s, 1970s, 1980s, and 1990s in the conterminous United States. Warm days are those ranked in the upper 10% of the 50-winter (JFM 1950–99) daily mean surface air temperature distribution. Dark (light) shaded areas indicate where the number of extremes is significantly greater (less) than the average number (based on the number of extremes per winter) at the 95% confidence level. The trend in the number of warm days [expressed as days yr^{-1} (50 yr^{-1})] is shown in the lower right.

remes is significantly greater (less) than average. Notice that this approach is based on the raw temperature distribution rather than an assumed analytical PDF. This is very important, since the temperature distribution is distinctly nonnormal at locations that are well removed from the midlatitude jet stream (e.g., the Gulf Coast region).

From the 1950s to the 1990s the number of warm days increased along the northern tier of states and in the West and decreased in the Southeast, but these

changes were not uniform (Fig. 5). For example, there was a large decrease in the number of warm days along the Gulf Coast from the 1950s to the 1960s, but relatively small changes since then. Cold days decreased in frequency in the western United States during the five-decade period, but again these changes were not uniform (Fig. 6). Cold days were especially frequent over the eastern half of the United States during the 1960s and 1970s. The trend in the total number of temperature extremes (i.e., warm plus cold days) is positive in the

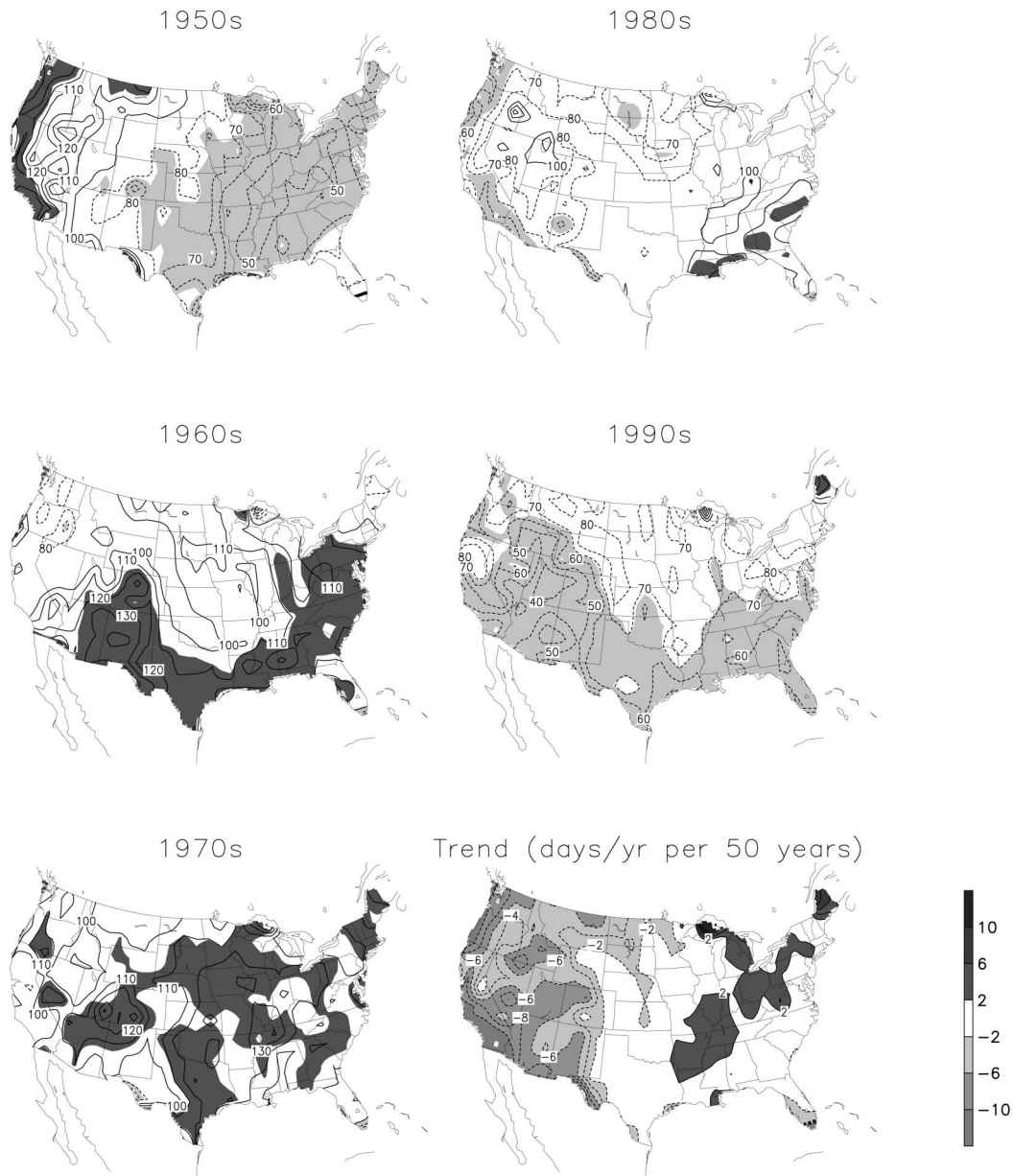


FIG. 6. Number of cold days that occurred during the 1950s, 1960s, 1970s, 1980s, and 1990s in the conterminous United States. Cold days are those ranked in the lower 10% of the 50-winter (JFM 1950–99) daily mean surface air temperature distribution. Dark (light) shaded areas indicate where the number of extremes is significantly greater (less) than the average number (based on the number of extremes per winter) at the 95% confidence level. The trend in the number of cold days [expressed as days yr^{-1} (50 yr^{-1})] is shown in the lower right.

northern United States (particularly in the upper Midwest) and negative in the southern United States (particularly along the Gulf Coast; Fig. 7). However, the largest number of extremes in any decade was observed during the 1970s over eastern portions of the country.

The average number of warm, cold, and warm plus cold days per decade (based on JFM 1950–99) is given in Table 2. The frequency of temperature extremes was computed locally, and then averaged for the conterminous United States. If temperature extremes are ran-

domly distributed, then the average number of warm, cold, and warm plus cold days per decade is 90, 90, and 180, respectively. The largest (smallest) number of warm days occurred during the 1990s (1960s) and the largest (smallest) number of cold days occurred during the 1970s (1990s). The 1970s had the largest total number of extremes (i.e., both warm and cold). The daily-mean temperature variance changes in a manner that is qualitatively consistent with the changes in the number of extremes in each decade (not shown).

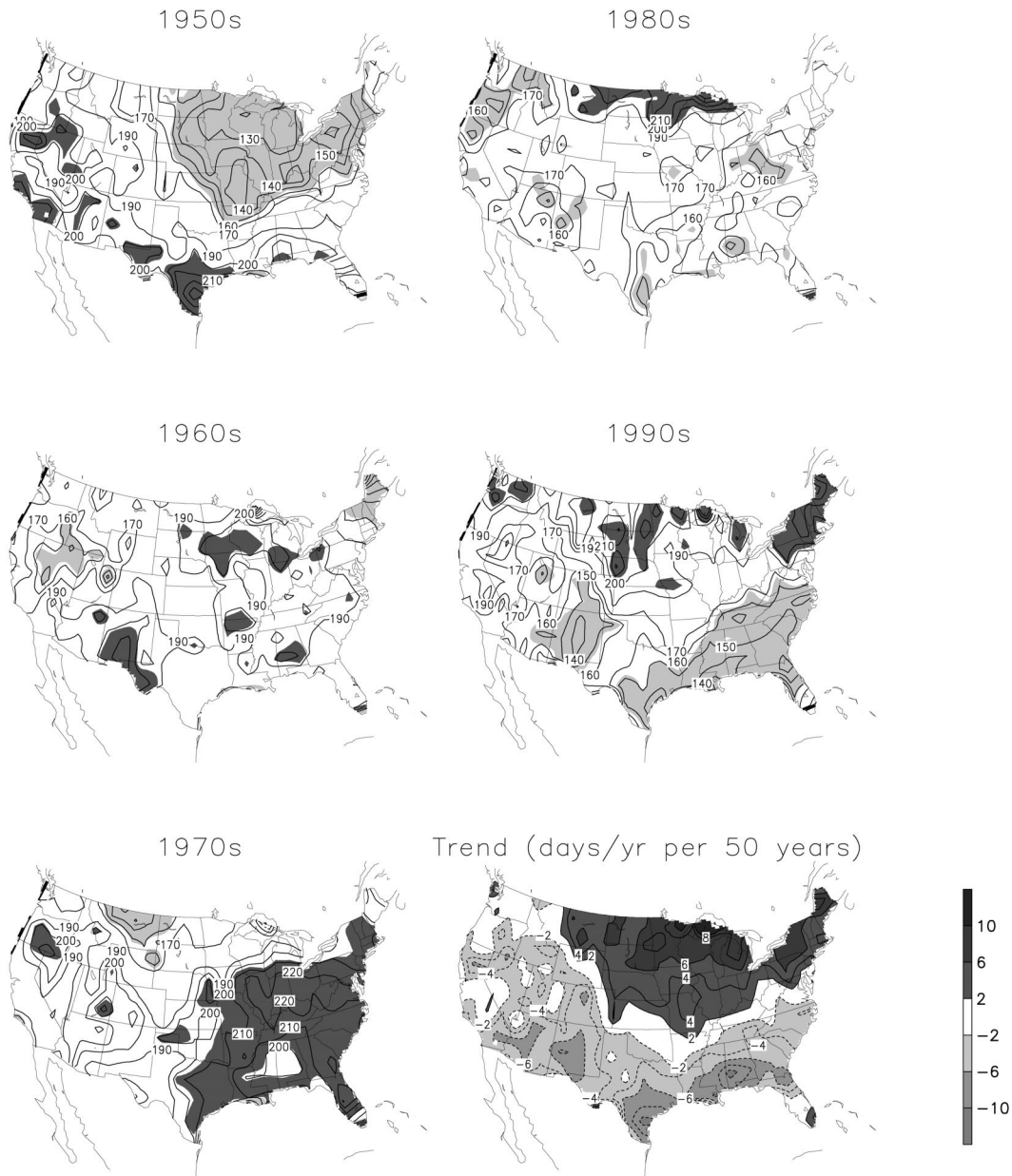


FIG. 7. Number of warm plus cold days that occurred during the 1950s, 1960s, 1970s, 1980s, and 1990s in the conterminous United States. Dark (light) shaded areas indicate where the number of extremes is significantly greater (less) than the average number (based on the number of extremes per winter) at the 95% confidence level. The trend in the number of temperature extremes [expressed as $\text{days yr}^{-1} (50 \text{ yr})^{-1}$] is shown in the lower right.

c. Linkage to the large-scale circulation

Winter 500-hPa height and anomaly patterns for each decade (Fig. 8) are qualitatively consistent with the patterns of temperature extremes discussed in the previous section (Figs. 5 and 6). During the 1950s the height anomaly pattern over the eastern North Pacific/North American region was dominated by the strong La Niña episode of the mid-1950s (resembles the negative phase of the PNA pattern). The 1960s and 1970s were a relatively cool period over much of North America and

characterized by an enhanced trough over the region (particularly during the 1970s). The height anomaly pattern during the 1970s also reflects the protracted La Niña episode during 1973–75. The 1980s and 1990s featured a weaker mean trough over much of North America that extended eastward across the midlatitudes of the North Atlantic. During this period the height anomaly pattern across the eastern North Pacific/North American region appears to reflect the increase in the frequency of El Niño episodes (resembles the positive phase of the PNA pattern). The trend in the 500-hPa height field (Fig. 8,

TABLE 2. Number of warm, cold, and warm plus cold days per decade during NH winter (based on JFM 1950–99) for the conterminous United States. The number of extremes was computed locally, and then area averaged for the conterminous United States. By definition, in an average decade there are 90 warm days, 90 cold days, and 180 warm and cold days, respectively. Values that are significantly greater (less) than average (based on departures from the average number of extremes per winter) at the 95% confidence level are indicated in bold.

Decade	Warm days	Cold days	Warm and cold days
1950s	91	82	173
1960s	78	106	184
1970s	84	111	195
1980s	88	85	173
1990s	111	67	178

lower right) also reflects this increase in El Niño episodes. The trend in the large-scale circulation features over the United States is qualitatively consistent with trends in the number of warm (Fig. 5) and cold (Fig. 6) temperature extremes. For example, the trend toward higher heights in the western United States in recent winters is qualitatively consistent with the increase in the number of warm days and the decrease in the number of cold days. The trend in the 500-hPa height anomaly pattern appears to be qualitatively consistent with the possible influence of more frequent El Niño episodes since the 1970s. A more thorough analysis is required to determine whether this trend is a consequence of the interplay between the decadal modes of climate variability such as the PDO (e.g., Mantua et al. 1997; Zhang et al. 1997).

5. Interannual climate variability and surface air temperature extremes

Standardized indices (i.e., normalized by standard deviation) representing ENSO (Fig. 1c) and the AO (Fig. 3c) are used together with composite analysis to relate interannual climate variability to surface air temperature extremes. We focus on how ENSO and the AO affect the winter mean temperature and how they influence the probabilities of extreme events on the tails of the distribution. High- and low-index phases of ENSO and the AO are used to produce composites; the high- (low-) index phases of each mode are deemed to occur when the appropriate index exceeds +0.5 (−0.5) standard deviations.

a. Winter temperature patterns and the leading modes

Typical La Niña and El Niño events are associated with significant regional temperature anomalies (Fig. 9, left column), but they tend to have relatively little impact on the seasonal mean temperature for the United States as a whole (i.e., regional anomalies tend to cancel over the course of a season). On the other hand, ENSO

influences the daily mean surface air temperature variance (see section 5b). Like ENSO, the AO is also associated with significant temperature anomalies, but they are of one sign at most locations and in the opposite sense depending on the phase (Fig. 9, right column). As a result, changes in the number of warm days associated with a particular AO phase are largely compensated for by changes in the number of cold days, so that the AO has relatively little influence on the daily mean surface air temperature variance (see section 5b).

b. Numbers of extreme events

As in section 4b, daily mean surface air temperature data were ranked (locally) from the warmest day to the coldest day for the period JFM 1950–99 and the warm (cold) days were defined as those in the upper (lower) 10% of the distribution. Recall that this implies that 9 warm (cold) days would occur at a particular location in an average 90-day winter. Warm (cold) days were then stratified based on whether they occurred during an El Niño, La Niña, or ENSO-neutral winter. Spatial patterns of the average number of temperature extremes per winter associated with each phase of ENSO are shown in Fig. 10. Warm, cold, and the combination of warm and cold days are shown in the left, center, and right columns, respectively.

Geographic patterns for the average number of warm and cold days during La Niña and El Niño (Fig. 10) are qualitatively consistent with the temperature anomaly patterns shown in the left column of Fig. 9. During La Niña winters the total number of temperature extremes increases along the Gulf Coast (primarily an increase in warm days) and in the intermountain West (primarily an increase in cold days). At most locations the number of winter temperature extremes is reduced during El Niño, especially along the southern tier of states (primarily a decrease in warm days). ENSO-neutral winters are characterized by an increase in the total number of extremes over much of the United States, especially in the Southwest and the Great Plains (primarily due to an increase in the number of warm days).

For the conterminous United States, La Niña and ENSO neutral are associated with an ~5% increase in the total number of extremes, while El Niño is associated with an ~10% decrease (Table 3). Thus, El Niño and La Niña influence the daily mean temperature variance in the United States, but have little impact on the U.S. mean temperature over the course of a season (see section 5a and Figs. 9 and 11). It is important to recognize, however, that the impacts of El Niño and La Niña on the atmospheric circulation, hence the day-to-day weather, vary during the annual cycle. Chen and Van den Dool (1997) found that La Niña impacts tend to weaken more rapidly during the late winter/early spring months than El Niño impacts. The linkage between ENSO and weather extremes for three-month running

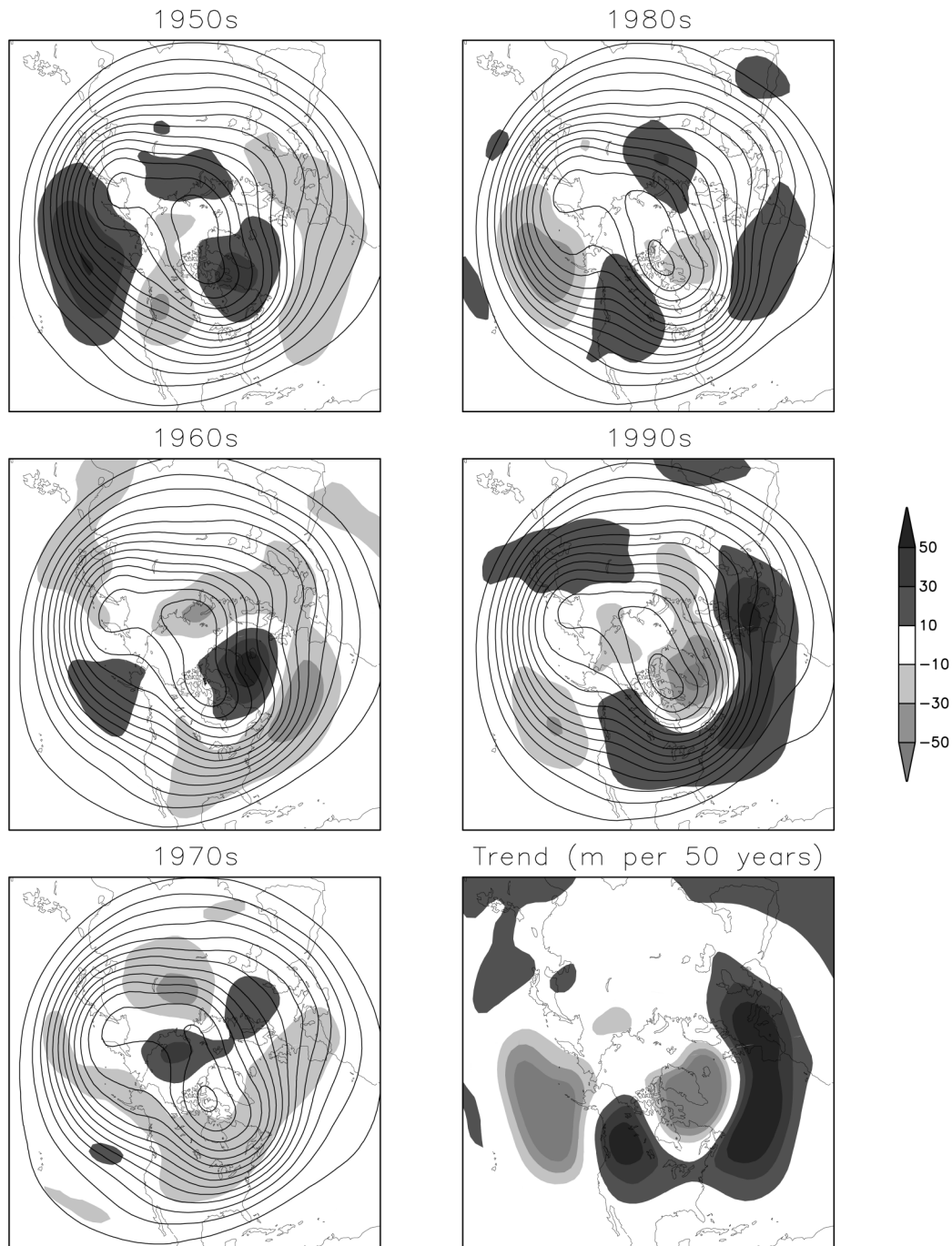


FIG. 8. 500-hPa height and anomalies during boreal winter (JFM) in the 1950s, 1960s, 1970s, 1980s, and 1990s. Anomalies are departures from 1950–99 base period monthly means. The trend in the 500-hPa height field [expressed as $\text{m} (50 \text{ yr})^{-1}$] is shown in the lower right.

seasons (i.e., JFM, FMA, MAM, etc.) has been examined by Zhou and Higgins (2001).

A comparison of the interannual (IA; timescales greater than 90 days) and intraseasonal (IS; timescales less than 90 days) variance of daily mean surface air temperature (Fig. 11, left and center columns, respectively) shows that the IS component dominates at all

locations in the conterminous United States. That is, the decrease in the likelihood of temperature extremes during El Niño relative to La Niña and ENSO neutral is primarily due to a decrease in the IS (i.e., day to day) variance (Fig. 11, right column).

The IS variance values tend to increase with latitude (i.e., inversely with mean temperature) (Fig. 11, center

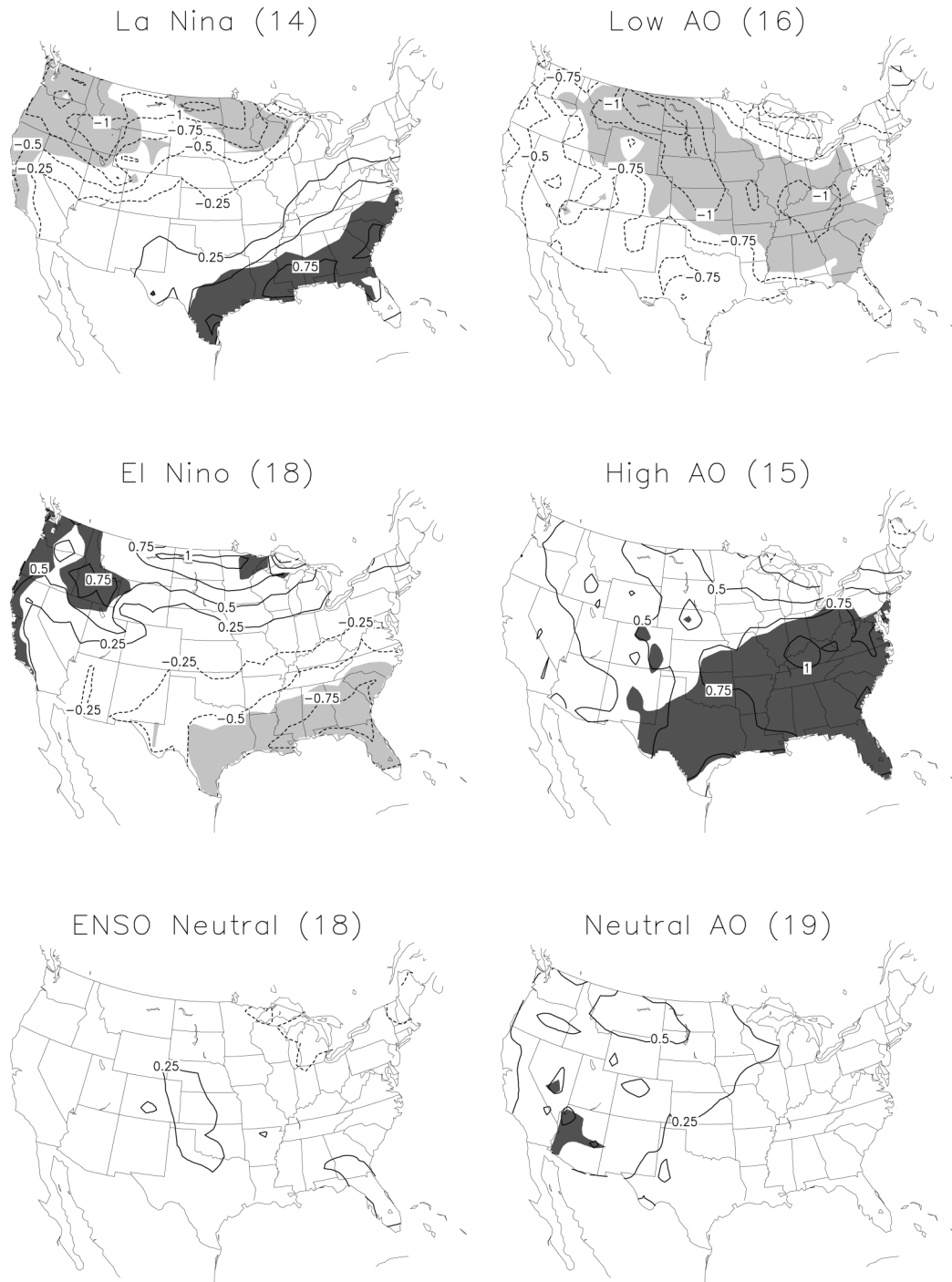


FIG. 9. Composite mean surface air temperature anomaly patterns for (left) La Niña, El Niño, and ENSO-neutral winters, and (right) low-AO, high-AO and AO-neutral winters during 1950–99. Temperature anomalies are referenced to a 1950–99 base period and are in units of $^{\circ}\text{C}$. The number of seasons included in each composite is indicated on the figure. Dark (light) shading indicates positive (negative) anomalies significant at the 95% confidence level.

column). The mean temperature always has greatest day-to-day variation in the lee of the Rockies and in the northern Great Plains during winter. There is high variability immediately east of the Rockies because of al-

ternations between arctic air intrusions, in which the cold air is often confined to the east of the Continental Divide, and chinook warmings that occur with zonal flow at upper levels (Barnston 1993). Proximity to the

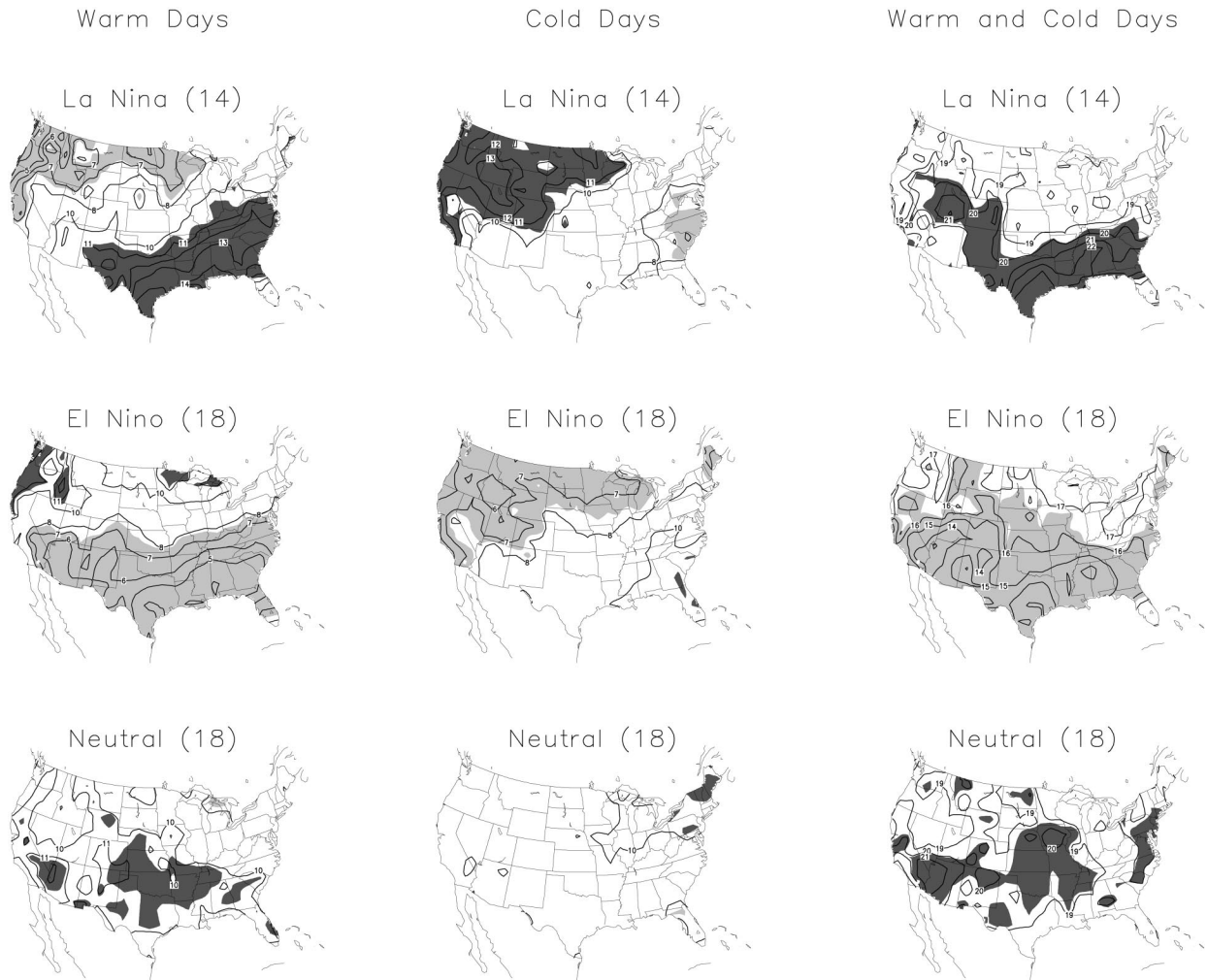


FIG. 10. Average number of daily mean surface air temperature extremes per winter associated with (top row) La Niña, (middle row) El Niño, and (bottom row) ENSO-neutral conditions. The left, center, and right columns show warm, cold, and warm plus cold daily temperature extremes, respectively. Warm (cold) days are those ranked in the upper (lower) 10% of the 50-winter (JFM 1950–99) daily mean surface air temperature distribution. The number of winters associated with each ENSO phase is indicated in parentheses. Dark (light) shaded areas indicate where the number of extremes is significantly greater (less) than the average number (based on the number of extremes per winter) at the 95% confidence level.

West Coast lowers variability due to the moderating influence of Pacific maritime air.

Changes in the IS variance associated with each ENSO phase are qualitatively consistent with changes

TABLE 3. Number of warm, cold, and warm plus cold days per winter for the conterminous United States during La Niña, El Niño, and ENSO-neutral winters. The number of extremes was computed locally, and then area averaged for the conterminous United States. By definition, in an average winter there are 9 warm days, 9 cold days, and 18 warm and cold days, respectively.

ENSO phase	Warm days	Cold days	Warm and cold days
La Niña	9	10	19
El Niño	8	8	16
ENSO neutral	10	9	19

in the tropospheric circulation. During La Niña the Pacific jet stream tends to be displaced to the north of its climatological mean position (Fig. 2a), resulting in a decrease in the frequency of arctic air intrusions into the northern Great Plains and Great Lakes regions. El Niño features a zonally extended Pacific jet stream that is situated to the south of its climatological mean position (Fig. 2b), resulting in a greater influx of Pacific maritime air into the western United States. During ENSO-neutral conditions, the Pacific jet stream is near its climatological mean position. Active polar and subtropical branches of the jet stream (Fig. 2c) result in increased temperature variance (e.g., an alternating sequence of cold air outbreaks and warmups).

Though the AO influences U.S. mean temperature, it has relatively little influence on the daily mean tem-

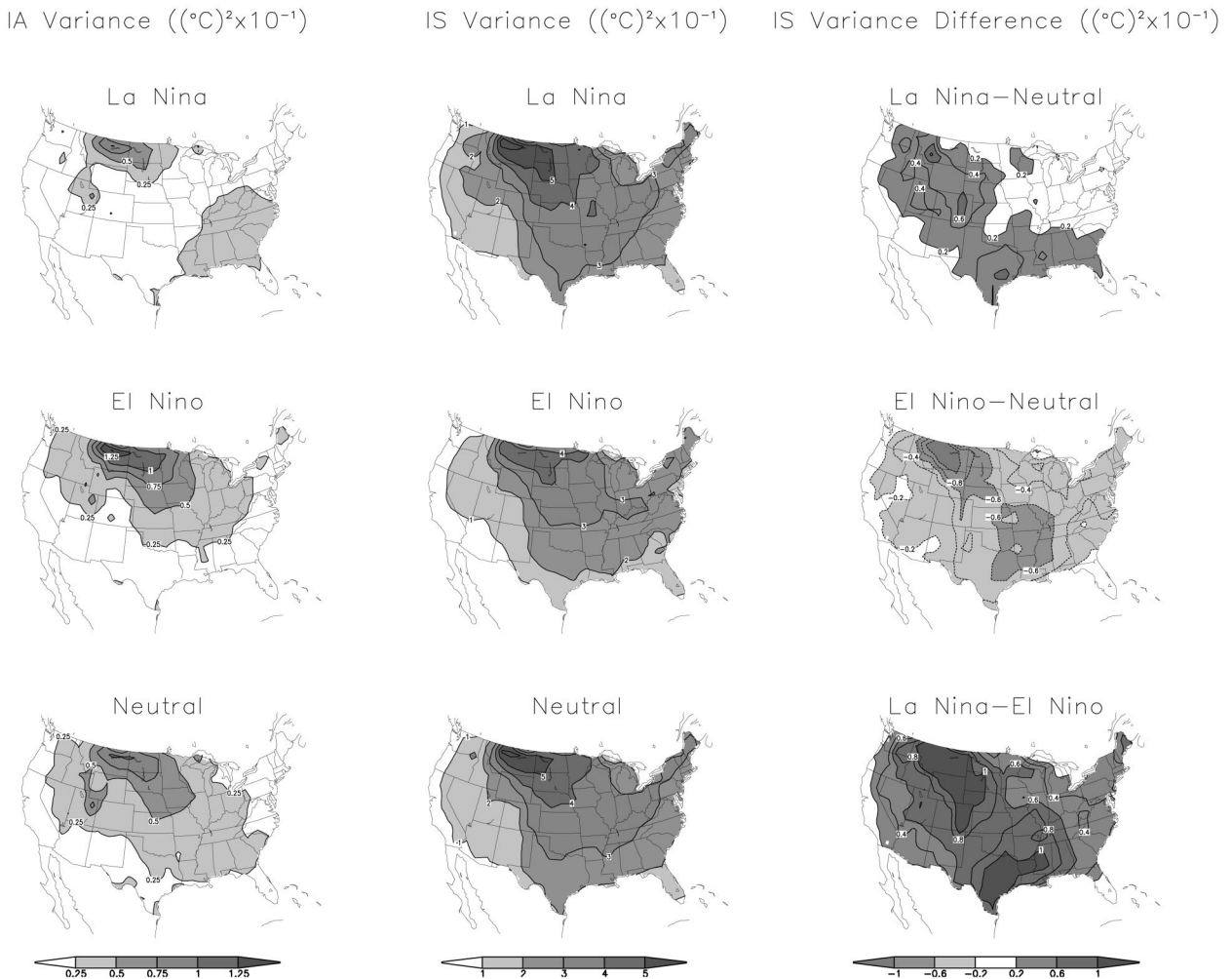


FIG. 11. Interannual (i.e., timescales greater than 90 days, IA) and intraseasonal (i.e., timescales less than 90 days, IS) components of the daily mean surface air temperature variance (left and center columns, respectively) for (top) La Niña, (middle) El Niño, and (bottom) ENSO-neutral winters during JFM 1950–99. The intraseasonal variance difference between ENSO phases is shown in the right column. In all cases the units are $(^{\circ}\text{C})^2 \times 10^{-1}$.

perature variance. Locally, changes in the number of warm days are compensated for by changes in the number of cold days in the opposite sense, so that the net change in the total number of temperature extremes is close to zero (Fig. 12). The low-index phase of the AO is associated with a decrease (an increase) in the number of warm (cold) days at most locations in the United States, while the opposite is true for the high-index phase of the AO. Thus, the low- (high) index phase of the AO acts to shift the temperature distribution toward colder (warmer) mean temperatures. However, the net change in the number of extremes (Fig. 12, right column) is small at most locations, and close to zero for the United States as a whole (Table 4). AO-neutral periods have little effect on the mean temperature and even less impact on the likelihood of extremes in the United States. Thus, the recent trend in the AO toward the high-

index phase (e.g., Thompson et al. 2000) is qualitatively consistent with the warming trend in U.S. surface air temperature in recent decades.

On a national basis, both the high- and low-index phases of the AO have less IS temperature variance than the AO-neutral phase. The variance of the daily AO index, in units of standard deviation, is +0.81, +0.85, and +0.92 for the high index, low index, and neutral phases, respectively; the differences between each of the phases are not statistically significant.

The geographical distributions of the coefficient of skewness (i.e., a measure of the third moment of the temperature distribution) were also examined. Skewness is a measure of the asymmetry of a distribution and is zero for a normal distribution. A distribution has positive skewness if the mean is greater than the mode (i.e., the most frequently occurring temperature), and nega-

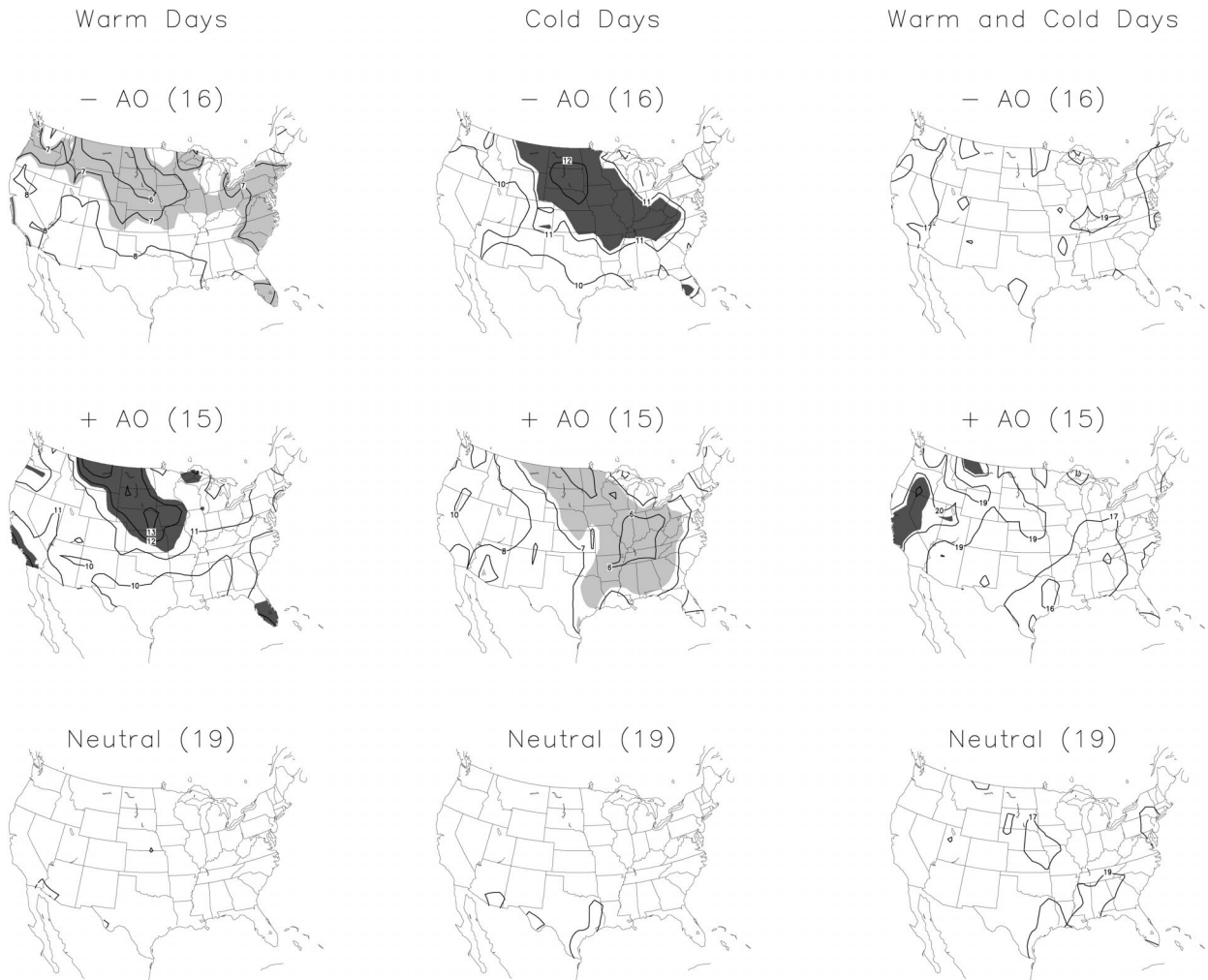


FIG. 12. Average number of daily mean surface air temperature extremes per winter associated with the (top) low- and (middle) high-index phases of the AO and with (bottom) AO-neutral conditions. The left, center, and right columns show warm, cold, and warm plus cold daily temperature extremes, respectively. Warm (cold) days are those ranked in the upper (lower) 10% of the 50 winter (JFM 1950–99) daily mean surface air temperature distribution. The number of winters associated with each phase is indicated in parentheses. Dark (light) shaded areas indicate where the number of extremes is significantly greater (less) than the average number (based on the number of extremes per winter) at the 95% confidence level.

tive skewness if the mean is less than the mode. Skewness in surface air temperature has been studied elsewhere (e.g., Van den Dool et al. 1978; Lehman 1987; Toth and Szentimrey 1990; Barnston 1993).

TABLE 4. Number of warm, cold, and warm plus cold temperature days per winter for the conterminous United States during high-AO, low-AO, and AO-neutral winters. The number of extremes was computed locally, and then area averaged for the conterminous United States. By definition, in an average winter there are 9 warm days, 9 cold days, and 18 warm and cold days, respectively.

AO phase	Warm days	Cold days	Warm and cold days
High AO	11	7	18
Low AO	7	11	18
Neutral AO	9	9	18

Negative skewness is found in regions where strong cold air intrusions occur only occasionally, such as the Pacific Northwest, Great Basin, and Rockies during La Niña (Fig. 13). Negative skewness is also found east of the Rockies in the southern and southeastern regions in the zone where cold air penetrates only with the strongest arctic outbreaks. This is especially the case during El Niño (Fig. 13). During El Niño, weak positive skewness is found over the Great Lakes region, as a result of occasional significant interruptions of the cold, cloudy conditions in this region. It is also found in coastal California, where unusually warm maximum temperatures may occur in the warm sector of Pacific storms. Positive skewness in the eastern United States during La Niña is related to the occasional passages of the warm sector of well-developed cyclones whose cen-



FIG. 13. Total skewness of daily mean surface air temperature for (top) La Niña, (middle) El Niño, and (bottom) ENSO-neutral winters during JFM 1950–99. Dark (light) shading indicates positive (negative) anomalies significant at the 95% confidence level.

ters pass to the northwest. Over the northwestern United States the temperature distribution exhibits large negative skewness during La Niña.

6. Discussion

The results demonstrate that linkages between climate variability and daily temperature extremes are pervasive, and hence that stronger collaboration between the modeling communities is needed to ensure that these linkages are properly captured in models. The examples presented here illustrate some of the physical phenomena that climate models must be able to simulate in order to be deemed credible for use in weather and climate forecasts and assessments. Systematic comparisons of weather and climate models and the observations are needed for forecast lead times beyond about a week, when climate impacts begin to dominate over the initialization used in weather forecasting. We note that Zhou and Higgins (2001, manuscript submitted to *J. Climate*) recently examined relationships between climate variability and the statistics of precipitation extremes in the United States using an approach similar to the one applied here.

It is important to recognize that there are other potentially important modes of climate variability that are likely to affect the United States, but many of the current datasets are too short to disentangle them; these include the Pacific Decadal Oscillation (PDO; e.g., Mantua et al. 1997), the quasi-70-yr near-interhemispheric variability of Delworth and Mann (2000), and the Atlantic multidecadal variability of Enfield and Mestas-Nunez (1999) among others. Folland et al. (1999) have identified a mode of variability similar to that of the above authors that has been used for operational forecasting in the Sahel since the late 1980s by the Met Office. All of these may contribute to further understanding of climate variability, and they are potentially important when trying to disentangle the regional effects of anthropogenic climate change from natural variability. Joint observational and modeling studies are needed to better identify the large-scale patterns of natural climate variability, and how these interact and/or change with long-term climate change. This approach is needed to distinguish the patterns of climate warming from the patterns of natural variability. In a follow-up study we will examine the links between climate variability and long-term trends in surface temperature with full consideration of the relevant multidecadal modes.

Acknowledgments. The authors are indebted to Huug Van den Dool and John Janowiak for careful reviews of a preliminary draft of this work and to three anonymous reviewers for valuable input that substantially improved the manuscript. The authors would also like to thank Dave Thompson and Mike Wallace for the AO index used in this study.

REFERENCES

- Barnston, A. G., 1993: *Atlas of Frequency Distribution, Autocorrelation and Cross-Correlation of Daily Temperature and Precipitation at Stations in the U.S., 1948–1991*. NOAA Atlas 11, 440 pp. [Available from Climate Prediction Center, World Weather Building, Rm. 605, 5200 Auth Rd., Camp Springs, MD 20746.]
- Bell, G. D., and V. E. Kousky, 1995: Diagnosing the midlatitude atmospheric response to ENSO. *Proc. 20th Annual Climate Diagnostics Workshop*, Seattle, WA, NOAA/Climate Prediction Center and JISAO, 9–12.
- Brown, B. G., R. W. Katz, and A. H. Murphy, 1986: On the economic value of seasonal precipitation forecasts: The following/planting problem. *Bull. Amer. Meteor. Soc.*, **67**, 833–841.
- Chen, W. Y., and H. M. Van den Dool, 1997: Atmospheric predictability of seasonal, annual, and decadal climate means and the role of the ENSO cycle: A model study. *J. Climate*, **10**, 1236–1254.
- Delworth, T. L., and M. E. Mann, 2000: Observed and simulated multidecadal variability in the Northern Hemisphere. *Climate Dyn.*, **16**, 661–676.
- Enfield, D. B., and A. M. Mestas-Núñez, 1999: Multiscale variabilities in global sea surface temperatures and their relationships with tropospheric climate patterns. *J. Climate*, **12**, 2719–2733.
- Folland, C. K., D. E. Parker, A. Colman, and R. Washington, 1999: Large scale modes of ocean surface temperature since the late nineteenth century. *Beyond El Niño: Decadal and Interdecadal Climate Variability*, A. Navarra, Ed., Springer-Verlag, 73–102.
- Gershunov, A., and T. P. Barnett, 1998: ENSO influence on intraseasonal extreme rainfall and temperature frequencies in the contiguous United States: Observations and model results. *J. Climate*, **11**, 1575–1586.
- Higgins, R. W., A. Leetmaa, Y. Xue, and A. Barnston, 2000: Dominant factors influencing the seasonal predictability of U.S. precipitation and surface air temperature. *J. Climate*, **13**, 3994–4017.
- Houghton, J. T., Y. Ding, D. J. Griggs, M. Noguer, P. J. van der Linden, and D. Xiaosu, Eds., 2001: *Climate Change 2001: The Scientific Basis: Contribution of Working Group I to the Third Assessment Report of the Intergovernmental Panel on Climate*. Cambridge University Press, 944 pp.
- Hurrell, J. W., 1995: Decadal trends in the North Atlantic Oscillation region temperatures and precipitation. *Science*, **269**, 676–679.
- Janowiak, J. E., G. D. Bell, and M. Chelliah, 1999: *A Gridded Data Base of Daily Temperature Maxima and Minima for the Conterminous United States: 1948–1993*. NCEP/Climate Prediction Center Atlas 6, 50 pp. [Available from the Climate Prediction Center, World Weather Building, Rm. 605, 5200 Auth Rd., Camp Springs, MD 20746.]
- Jones, P. D., 1994: Hemispheric surface air temperature variations: A reanalysis and an update to 1993. *J. Climate*, **7**, 1794–1802.
- Kalnay, E., and Coauthors, 1996: The NCEP/NCAR 40-Year Reanalysis Project. *Bull. Amer. Meteor. Soc.*, **77**, 437–471.
- Lehman, R. L., 1987: Probability distributions of monthly degree day variables at U.S. stations. Part I: Estimating the mean value and variance from temperature data. *J. Climate Appl. Meteor.*, **26**, 329–340.
- Livezey, R. E., and T. M. Smith, 1999: Covariability of aspects of North American climate with global sea surface temperatures on interannual to interdecadal timescales. *J. Climate*, **12**, 289–302.
- Mantua, N. J., S. R. Hare, Y. Zhang, J. M. Wallace, and R. C. Francis, 1997: A Pacific interdecadal climate oscillation with impacts on salmon production. *Bull. Amer. Meteor. Soc.*, **78**, 1069–1079.
- Pan, W. H., L. A. Li, and M. J. Tsai, 1995: Temperature extremes and mortality from coronary heart disease and cerebral infarction in elderly Chinese. *Lancet*, **345**, 353–355.
- Redmond, K. T., and D. R. Cayan, 1994: El Niño/Southern Oscillation and western climate variability. Preprints, *Sixth Conf. on Climate Variations*, Nashville, TN, Amer. Meteor. Soc., 141–145.
- Reynolds, R. W., and T. M. Smith, 1995: A high resolution global sea surface temperature climatology. *J. Climate*, **8**, 1571–1583.
- Ropelewski, C. F., and M. S. Halpert, 1986: North American precipitation and temperature patterns associated with the El Niño/Southern Oscillation (ENSO). *Mon. Wea. Rev.*, **114**, 2352–2362.
- , and —, 1996: Quantifying Southern Oscillation–Precipitation relationships. *J. Climate*, **9**, 1043–1059.
- Smith, C. A., and P. Sardeshmukh, 1999: The effect of ENSO on the intraseasonal variance of surface temperature in winter. *Int. J. Climatol.*, **20**, 1543–1557.
- Smith, T. M., R. W. Reynolds, R. E. Livezey, and D. C. Stokes, 1996: Reconstruction of historical sea surface temperatures using empirical orthogonal functions. *J. Climate*, **9**, 1403–1420.
- Thompson, D. W. J., and J. M. Wallace, 1998: The Arctic Oscillation signature in the wintertime geopotential height and temperature fields. *Geophys. Res. Lett.*, **25**, 1297–1300.
- , and —, 2000: Annular modes in the extratropical circulation. Part I: Month-to-month variability. *J. Climate*, **13**, 1000–1016.
- , —, and G. C. Hegerl, 2000: Annular modes in the extratropical circulation. Part II: Trends. *J. Climate*, **13**, 1018–1036.
- Toth, Z., and Z. Szentimrey, 1990: The binormal distribution: A distribution for representing asymmetrical but normal-like weather elements. *J. Climate*, **3**, 128–136.
- Van den Dool, H. M., H. J. Krijnen, and C. J. E. Schuurmans, 1978: Average winter temperatures at De Bilt (The Netherlands): 1634–1977. *Climatic Change*, **1**, 319–329.
- van Loon, H., and J. C. Rogers, 1978: Seesaw in winter temperatures between Greenland and northern Europe. Part I: General description. *Mon. Wea. Rev.*, **106**, 296–310.
- Walker, G. T., and E. W. Bliss, 1932: World Weather V. *Mem. Roy. Meteor. Soc.*, **4**, 53–83.
- Wallace, J. M., 2000: North Atlantic Oscillation/Northern Hemisphere annular mode: Two paradigms—One phenomenon. *Quart. J. Roy. Meteor. Soc.*, **126**, 791–806.
- Zhang, Y., J. M. Wallace, and D. S. Battisti, 1997: ENSO-like interdecadal variability: 1900–93. *J. Climate*, **10**, 1004–1020.
- Zhou, Y., and R. W. Higgins, 2001: *Relationships between El Niño–Southern Oscillation and the Arctic Oscillation: A Climate–Weather Link*. NCEP/Climate Prediction Center Atlas 8. [Available online at <http://www.cpc.ncep.noaa.gov/products/outreach/atlas.html>.]